1 **Normal pancreatic β-cell function in mice with *RIP-Cre*-mediated inactivation of**

2 **p62/SQSTM1**

3

4 **Running title:** Role of p62/SQSTM1 in β-cell function

5

6 Akira Honda,[1] Koji Komiya,[1] Akemi Hara,[1,2] Ayako Fukunaka,[1,5] Luka Suzuki,[1]

7 Takeshi Miyatsuka,[1,2] Takeshi Ogihara,[1] Yoshio Fujitani,[1,5] and Hirotaka Watada[1,2,3,4]

8

9 [1]Department of Metabolism and Endocrinology, [2]Center for Identification of Diabetic

10 Therapeutic Targets, [3]Center for Therapeutic Innovations in Diabetes, and [4]Sportology

11 Center, Juntendo University Graduate School of Medicine, Tokyo, 113-8421, Japan,

12 [5]Laboratory of Developmental Biology and Metabolism, Institute for Molecular and

13 Cellular Regulation, Gunma University, Maebashi 371-8512, Japan

14

15

17

Correspondence to: Yoshio Fujitani, M.D., Ph.D., Laboratory of Developmental

Biology & Metabolism, Institute for Molecular & Cellular Regulation, Gunma

University, 3-39-15 Showa-machi, Maebashi 371-8512, Japan, E-mail:

fujitani@gunma-u.ac.jp; or Hirotaka Watada, M.D., Ph.D., Department of Metabolism

and Endocrinology, Juntendo University Graduate School of Medicine, 2-1-1 Hongo,

Bunkyo-ku, Tokyo 113-8421, Japan, E-mail: hwatada@juntendo.ac.jp

24

25

26 **Abstract**

27 Recent studies have suggested that decreased pancreatic β-cell function and mass are

28 common features of patients with type 2 diabetes mellitus. Pancreatic β-cell

29 homeostasis is regulated by various types of signaling molecules and stress responses.

30 Sequestosome 1/p62 (SQSTM1, hereafter referred to as p62) is a ubiquitin-binding

31 adaptor protein involved in cell signaling, oxidative stress, and autophagy. Because

32 p62 appears to play an important role in maintaining mitochondrial quality control, it is

33 possible that the loss of *p62* in pancreatic β cells contributes to mitochondrial

34 dysfunction, and thus leading to impaired glucose tolerance. In this study we

35 investigated the physiological roles of p62 by inactivating *p62* in a β-cell specific

36 manner. We found that firstly, rat insulin-2 promoter-*Cre* (*RIP-Cre*)-mediated *p62*

37 inactivation did not cause body weight gain, although ubiquitous inactivation of *p62*

38 was previously shown to result in severe obesity. Secondly, we found no gross

39 structural disorganization of the islets of *p62*-deficient mice. Consistent with normal

40 islet morphology, no impairment in glucose tolerance was observed in mice with

41   *RIP-Cre*-mediated *p62* deletion. These results suggest that *p62* is dispensable for

42   normal islet organization and β-cell function.

43

Introduction

44

45   Type 2 diabetes mellitus is a metabolic disorder characterized by hyperglycemia

46   resulting from the complex interplay of multiple genetic and environmental factors,

47   resulting in both decreased insulin action on target tissues and defective pancreatic

48   β-cell insulin secretion in response to glucose [1]. The natural history of diabetes is

49   strongly associated with the disability of pancreatic β cells to adapt to meet the

50   increased demand for insulin secretion caused by increased insulin resistance [2].

51   Therefore, elucidating the molecular mechanisms underlying pancreatic β-cell

52   dysfunction is a key to understanding the pathology of diabetes [3,4].

53   Sequestosome 1 (SQSTM1, referred to hereafter as p62) is a multifunctional

54   scaffold protein that can interact with several signaling pathways through its functional

55   subdomains, including the Phox and Bem1 (PB1) domain, zinc-finger domain, TNF

56   receptor-associated factor 6 (TRAF6)-binding domain, and Kelch-like ECH-associated

57   protein 1 (Keap1) interacting region (KIR) [5-7]. p62/SQSTM1 can activate the

58   antioxidant response by interacting with the Keap1-Nrf2 pathway [8-10]. The

59   Keap1-Nrf2 antioxidant response pathway is one of the major cellular defense

60 mechanisms against oxidative insults [11,12]. p62/SQSTM1 also contains a ubiquitin

61 association domain and LC3-interacting region, and is thus selectively degraded by

62 autophagy together with ubiquitinated proteins that are recruited to autophagosomes

63 via p62 [13,14]. Based on the assumption that the degradation of p62 largely depends

64 on autophagy, the accumulation of cellular p62 has been widely used as a diagnostic

65 marker for autophagic failure [15]. In fact, p62 accumulates in tissues such as liver,

66 brain, and heart under autophagy-deficient conditions [16-18].

67   p62 has been reported to play a crucial role in the regulation of metabolism in

68 white adipose tissue and liver. Mice with global inactivation of *p62* (*p62*^{-/-}) were found

69 to develop mature-onset obesity and several features of metabolic syndrome, including

70 excess fat accumulation in white adipose tissue and liver, impaired glucose tolerance,

71 and insulin sensitivity [19]. A subsequent study on brain-specific *p62* knockout mice

72 demonstrated that a lack of *p62* in the brain causes leptin resistance, thereby leading to

73 hyperphagia and obesity [20]. The p62 protein is also involved in several

74 ageing-related pathologies. *p62*^{-/-} mice have a reduced lifespan and show premature

75 aging phenotypes with increased mitochondrial damage and dysfunction [21]. Given

76   the importance of p62 in maintaining mitochondrial homeostasis through the

77   autophagic degradation of damaged mitochondria, or so called mitophagy, it is

78   possible that loss of *p62* in pancreatic β cells contributes to mitochondrial dysfunction

79   and thereby reduces insulin release, resulting in impaired glucose tolerance [5]. On the

80   other hand, a recent study reported that in contrast to what has been reported for

81   ubiquitin-induced pexophagy and xenophagy, p62 appears to be dispensable for

82   mitophagy [22]. The same study also reported that mitochondrial-anchored ubiquitin is

83   sufficient to recruit p62 to mitochondria and promote mitochondrial clustering, but

84   does not promote mitophagy, further demonstrating the controversy regarding the role

85   of p62 in the mitochondrial homeostasis of β cells. Therefore, in this study, as the first

86   step towards elucidating the role of p62 itself in β cells, we investigated the effects of

87   β-cell-specific *p62* ablation on β-cell function.

88

89 **Materials and Methods**

90

91 *Animal experiments*

92 All mice were housed in specific pathogen-free barrier facilities, maintained under a

93 12-hour light/12-hour dark cycle, and provided standard rodent food (Oriental Yeast,

94 Tokyo, Japan) and water *ad libitum*. Rat insulin 2 promoter-driven Cre recombinase

95 [23] was used to delete *p62* in a pancreatic β-cell-specific manner. The generation of

96 $p62^{flox/+\ (f/+)}$ mice was performed as described previously [20]. *RIP-Cre* mice were

97 crossed with $p62^{f/+}$ mice to generate $p62^{f/+}$*:RIP-Cre* mice. Next, $p62^{f/+}$ mice were

98 crossed with $p62^{f/+}$*:RIP-Cre* mice to generate $p62^{f/f}$*:RIP-Cre* mice.

99

100 *Measurement of blood glucose and insulin levels*

101 To measure non-fasting glucose levels, glucose levels were measured in the morning.

102 For the intraperitoneal glucose tolerance test (IPGTT), after an overnight fast (16 h),

103 age-matched 22-week-old male mice were injected intraperitoneally with glucose (0.5

104 g/kg body weight). A few microliters of blood were taken from the tail vein of awake

105   mice, and glucose levels were measured using whole blood with a compact glucose

106   analyzer (ACCU-CHEK® Compact Plus, Roche Diagnostics, Basel, Switzerland) at

107   the indicated time points. To measure insulin levels, whole blood samples were

108   collected from the orbital sinus in awake mice and centrifuged. After centrifugation,

109   plasma was stored at −80 °C until analysis. Insulin levels were measured using an

110   enzyme-linked immunosorbent assay kit (Morinaga Co., Kanagawa, Japan).

111

112   ***Isolation of mouse islets***

113   After anesthetization of mice and euthanasia by cutting of their carotid arteries, the

114   distal ends of the common bile duct were clamped adjacent to the duodena.

115   Subsequently, common bile ducts were cannulated with a 30-G needle near the liver.

116   Acinar tissue was disrupted by injecting 1.5 mL of a 0.15% collagenase solution. Then,

117   pancreata were removed, and incubated in 1 mL of 0.15% collagenase solution for 40

118   min at 37 °C. For isolating islets from the digested acinar tissue, pancreata were

119   shaken for 1 min in conical tubes with 40 mL Hank's balanced salt solution (HBSS).

120   Next, solutions were incubated for 90 sec until the islets sunk to the bottom of the tube.

121   Then, supernatants were aspirated and 50 mL of HBSS was added. This cycle of

122   incubating, aspirating, and adding was continued until the solution became clear. The

123   islets were transferred to dishes and collected using a micropipette under a dissecting

124   microscope.

125

126   ***RT-PCR analysis***

127   Total RNA was extracted from isolated islets using RNeasy Plus Mini Kit (Qiagen,

128   Valencia, CA, USA), and cDNA was synthesized using Ovation RNA Amplification

129   System V2 (Nugen, San Carlos, CA, USA) according to the manufacturer's protocols.

130   Real-time PCR was performed using TaqMan Custom Arrays (Applied Biosystems,

131   Foster City, CA, USA). The expression levels of *Sqstm1/p62* (Mm00448091_m1)

132   mRNAs were quantified by TaqMan Real-Time PCR Assays (Applied Biosystems,

133   Foster City, CA, USA), and normalized to *glucuronidase beta* (*Gusb*,

134   Mm01197698_m1). Data are expressed as the mean ± SE.

135

136   ***Immunohistochemistry and morphometric analysis***

137 After anesthetization, 22-week-old mice were thoroughly perfused with saline

138 followed by 4% paraformaldehyde. Pancreata were removed and fixed with 4%

139 paraformaldehyde for at least 2 days at 4 °C until embedding. Fixed tissues were

140 embedded in paraffin and then cut into 4-μm-thick sections and mounted onto slides.

141 The sections were blocked with 2% bovine serum albumin for 30 min at room

142 temperature, and then incubated with each primary antibody overnight at 4 °C. The

143 primary antibody for guinea pig anti-human insulin (Dako, Glostrup, Denmark) was

144 diluted to 1:1,000 in 2% bovine serum albumin. The streptavidin-biotin complex

145 method was used for detection, and hence the sections were incubated with

146 biotinylated goat anti-guinea pig IgG (1:1,000) secondary antibody for 60 min at room

147 temperature. β-cell areas were determined using five insulin-stained sections from each

148 mouse, and each section was separated by at least 200 μm to avoid double scoring of

149 the same islet. Images of pancreatic tissue were captured using a microscope

150 (BZ-9000; Keyence, Osaka, Japan). Areas of insulin-stained pancreatic islets were

151 determined automatically using image analysis software (WinROOF; Mitani Corp.,

152 Fukui, Japan).

153

154   *Statistical analyses*

155   All quantitative data are reported as the mean ± SEM. Statistical analyses were

156   performed using the unpaired two-tailed Student t-test or nonrepeated ANOVA. A

157   p-value of less than 0.05 was considered to indicate a significant difference between

158   groups.

159

160   *Ethical approval*

161   The animal experiment protocol was approved by the Ethics Review Committee of

162   Animal Experimentation of Juntendo University.

163
164

165 **Results**

166   To analyze the physiological roles of *p62* in pancreatic β cells, *p62$^{f/f}$:RIP-Cre* mice

167   were generated by crossing *p62$^{f/f}$* mice with *p62$^{f/+}$:RIP-Cre* mice. Quantitative

168   RT-PCR analysis indicated that *p62* mRNA levels of *p62$^{f/f}$:RIP-Cre* (referred to

169   hereafter as *p62$^{f/f}$:Cre*) islets were reduced by more than 70% of that of *p62$^{+/+}$:Cre*

170   islets (Fig. 1). Given that β cells constitute 70% of normal islet cells [24] and the

171   recombination efficiency of *RIP-Cre* is reported to be 80%-90% [25], p62 expression

172   was efficiently eliminated from β cells in *p62$^{f/f}$:Cre* islets. No gross abnormalities were

173   observed in *p62$^{f/f}$:Cre* mice. In contrast to the body weight gain observed in ubiquitous

174   *p62*-knockout mice [19] and brain-specific *p62*-knockout mice [20], *p62$^{f/f}$:Cre* mice

175   were indistinguishable in body weight from age-matched control *p62$^{+/+}$:Cre*

176   littermates between the ages of 6 and 22 weeks (Fig. 2A). There was no difference in

177   non-fasting blood glucose levels between the two groups (Fig. 2B). The glucose

178   tolerance test (GTT) indicated no deterioration of glucose tolerance in *p62$^{f/f}$:Cre* mice

179   (Fig. 3A). During the GTT, a normal insulin secretion profile was observed, which was

180   comparable to that of *p62$^{+/+}$:Cre* mice (Fig. 3B). Moreover, histological analysis

181   demonstrated that there were no apparent morphological abnormalities or degenerative

182   changes in the islets of *p62*-deficient mice (Fig. 4A). There was no significant change

183   in islet cell mass, assessed by insulin immunostaining, in *p62$^{f/f}$:Cre* mice compared

184   with *p62$^{+/+}$:Cre* mice (Fig. 4B, C). The normal β-cell mass observed in β-cell-specific

185   *p62*-deficient mice is consistent with the normal β-cell proliferation in response to

186   inceased insulin resistance observed in global p62-deficient mice. Taken together, we

187   conclude that there are no differences between β-cell-specific *p62*-deficient mice and

188   control mice in terms of body weight, non-fasting blood glucose levels, glucose

189   tolerance, islet cell mass, and β-cell morphology. These results indicate that

190   p62/SQSTM1 in pancreatic β cells is dispensable for normal islet architecture, normal

191   glucose tolerance, and β-cell function.

192

193

194 **Discussion**

195 Ubiquitous inactivation of *p62* (*p62*$^{-/-}$) has been reported to result in early onset

196 glucose intolerance and maturity-onset obesity [19]. Our results further confirmed that

197 impaired glucose tolerance in *p62*$^{-/-}$ mice is primarily due to peripheral insulin

198 resistance, excluding the possible involvement of *p62* function in pancreatic β cells.

199 *p62*$^{-/-}$ mice develop insulin resistance before their obesity becomes apparent [19]. *p62*$^{-/-}$

200 mice have increased fat content due to the hyperactivation of ERK, which causes

201 adipogenesis and obesity. At the molecular level, it has been demonstrated that p62

202 controls adipogenesis by inhibiting ERK activation via a direct interaction [19]. In

203 contrast to such a cell-autonomous role of p62 in adipocyte differentiation, our study

204 highlights the dispensable role of p62 in normal β-cell function and homeostasis, at

205 least when mice are fed a normal diet.

206　　　　As p62 appears to play an important role in maintaining mitochondrial quality

207 control through mitophagy, it is possible that the loss of *p62* in pancreatic β cells may

208 cause mitochondrial dysfunction and thus result in impaired glucose tolerance [5].

209 Normal β-cell function and mass in β-cell-specific *p62*-deficient mice suggested

210 redundant autophagy receptors; for instance, NBR1, which shares similar functional

211 domains with p62, may have a compensatory role in mitophagy when p62 is deficient

212 [26]. However, a recent study reported that NBR1 is dispensable for PARK2-mediated

213 mitophagy regardless of the presence or absence of p62 [27]. Thus, other mitophagy

214 receptors, such as BCL2L13 and FKBP8, may be involved in the autophagic

215 degradation of damaged mitochondria [28, 29]. Further studies will hence be needed to

216 determine the molecules that may compensate for p62 in *p62$^{f/f}$:RIP-Cre* mice.

217   Harada et al. reported that brain-specific *p62* disruption by *nestin-Cre* results in

218 significant body weight gain compared with control mice at 20 weeks of age [20].

219 Importantly, pair feeding completely abolished the obese phenotype of brain-specific

220 *p62* KO mice, indicating that p62 in the brain inhibits appetite and thus controls body

221 weight homeostasis [20]. It has been demonstrated that *RIP-Cre* is expressed in a

222 subset of neurons in the hypothalamus, and that deletion of Stat3 results in progressive

223 obesity [30]. We found that *p62$^{f/f}$:RIP-Cre* mice show no noticeable obesity,

224 suggesting that p62 function in a brain area other than the *Rip-Cre*-expressing area is

225 important for appetite regulation.

226   We previously reported that autophagy deficiency in β cells is associated with

227   β-cell dysfunction [31]. Mice with β-cell specific autophagy deficiency

228   (*Atg7^{f/f}:RIP-Cre*) showed impaired glucose tolerance with abnormal β-cell

229   morphology. In that study, a large amount of p62 accumulation was observed. It has

230   been reported that the liver injury occurring in liver-specific autophagy-deficient mice

231   is largely suppressed by the concomitant loss of *p62*, indicating that liver injury is

232   caused by a p62-dependent mechanism [14]. In contrast, the molecular mechanisms as

233   to how β cells are damaged under autophagy deficiency is largely unknown. Here we

234   show that the loss of p62 in pancreatic β cells does not affect their morphology or

235   function. Therefore, future studies should focus on investigating whether the

236   accumulation of p62/SQSTM1 contributes to β-cell failure under autophagy-deficient

237   conditions, by generating β-cell specific *Atg7/p62* double KO mice.

238

239 **Conflicts of Interest**

240

241 All authors report no conflicts of interest.

242

243

References

254   **References**

255

256   1.   American Diabetes Association (2009) Diagnosis and classification of diabetes
257   mellitus. *Diabetes Care* 32 Suppl 1: S62-67.

258   2.   Kahn SE (2003) The relative contributions of insulin resistance and beta-cell
259   dysfunction to the pathophysiology of Type 2 diabetes. *Diabetologia* 46: 3-19.

260   3.   Halban PA, Polonsky KS, Bowden DW, Hawkins MA, Ling C, *et al.* (2014)
261   β-cell failure in type 2 diabetes: postulated mechanisms and prospects for
262   prevention and treatment. *J Clin Endocrinol Metab* 99: 1983-1992.

263   4.   Prentki M, Nolan CJ (2006) Islet β cell failure in type 2 diabetes. *J Clin Invest*
264   116: 1802-1812.

265   5.   Bitto A, Lerner CA, Nacarelli T, Crowe E, Torres C, *et al.* (2014)
266   P62/SQSTM1 at the interface of aging, autophagy, and disease. *Age (Dordr)*
267   36: 9626.

268   6.   Katsuragi Y, Ichimura Y, Komatsu M (2015) p62/SQSTM1 functions as a
269   signaling hub and an autophagy adaptor. *FEBS J* 282: 4672-4678.

270   7.   Nezis IP, Stenmark H (2012) p62 at the interface of autophagy, oxidative stress
271   signaling, and cancer. *Antioxid Redox Signal* 17: 786-793.

272   8.   Komatsu M, Kurokawa H, Waguri S, Taguchi K, Kobayashi A, *et al.* (2010)
273   The selective autophagy substrate p62 activates the stress responsive
274   transcription factor Nrf2 through inactivation of Keap1. *Nat Cell Biol* 12:
275   213-223.

276   9.   Lau A, Wang XJ, Zhao F, Villeneuve NF, Wu T, *et al.* (2010) A noncanonical
277   mechanism of Nrf2 activation by autophagy deficiency: direct interaction
278   between Keap1 and p62. *Mol Cell Biol* 30: 3275-3285.

279   10.   Copple IM, Lister A, Obeng AD, Kitteringham NR, Jenkins RE, *et al.* (2010)
280   Physical and functional interaction of sequestosome 1 with Keap1 regulates the
281   Keap1-Nrf2 cell defense pathway. *J Biol Chem* 285: 16782-16788.

282 11. Taguchi K, Motohashi H, Yamamoto, M. (2011) Molecular mechanisms of the
283   Keap1-Nrf2 pathway in stress response and cancer evolution. *Genes Cells* 16:
284   123-140.

285 12. Kansanen E, Kuosmanen SM, Leinonen H, Levonen AL (2013) The
286   Keap1-Nrf2 pathway: Mechanisms of activation and dysregulation in cancer.
287   *Redox Biol* 1:45-49.

288 13. Bjorkoy G, Lamark T, Brech A, Outzen H, Perander M, *et al.* (2005)
289   p62/SQSTM1 forms protein aggregates degraded by autophagy and has a
290   protective effect on huntingtin-induced cell death. *J Cell Biol* 171: 603-614.

291 14. Komatsu M, Waguri S, Koike M, Sou YS, Ueno T, *et al.* (2007) Homeostatic
292   levels of p62 control cytoplasmic inclusion body formation in
293   autophagy-deficient mice. *Cell* 131: 1149-1163.

294 15. Klionsky DJ, Abdelmohsen K, Abe A, Abedin MJ, Abeliovich H, *et al.* (2016)
295   Guidelines for the use and interpretation of assays for monitoring autophagy
296   (3rd edition). *Autophagy* 12:1-222.

297 16. Komatsu M, Waguri S, Ueno T, Iwata J, Murata S, *et al.* (2005) Impairment of
298   starvation-induced and constitutive autophagy in Atg7-deficient mice. *J Cell
299   Biol* 169: 425-434.

300 17. Hara T, Nakamura K, Matsui M, Yamamoto A, Nakahara Y, *et al.* (2006)
301   Suppression of basal autophagy in neural cells causes neurodegenerative
302   disease in mice. *Nature* 441: 885-889.

303 18. Nakai A, Yamaguchi O, Takeda T, Higuchi Y, Hikoso S, *et al.* (2007) The role
304   of autophagy in cardiomyocytes in the basal state and in response to
305   hemodynamic stress. *Nat Med* 13: 619-624.

306 19. Rodriguez A, Duran A, Selloum M, Champy MF, Diez-Guerra FJ, *et al.* (2006)
307   Mature-onset obesity and insulin resistance in mice deficient in the signaling
308   adapter p62. *Cell Metab* 3: 211-222.

309 20. Harada H, Warabi E, Matsuki T, Yanagawa T, Okada K. *et al.* (2013)
310   Deficiency of p62/Sequestosome 1 causes hyperphagia due to leptin resistance
311   in the brain. *J Neurosci* 33: 14767-14777.

312   21. Kwon J, Han E, Bui CB, Shin W, Lee J, *et al.* (2012) Assurance of
313   mitochondrial integrity and mammalian longevity by the
314   p62-Keap1-Nrf2-Nqo1 cascade. *EMBO Rep* 13: 150-156.

315   22. Narendra D, Kane LA, Hauser DN, Fearnley IM, Youle, RJ (2010)
316   p62/SQSTM1 is required for Parkin-induced mitochondrial clustering but not
317   mitophagy; VDAC1 is dispensable for both. *Autophagy* 6: 1090-1106.

318   23. Gannon M, Shiota C, Postic C, Wright CV, Magnuson M (2000) Analysis of
319   the Cre-mediated recombination driven by rat insulin promoter in embryonic
320   and adult mouse pancreas. *Genesis* 26: 139-142.

321   24. Rhodes CJ (2005) Type 2 diabetes-a matter of β-cell life and death? *Science*
322   307:380-384.

323   25. Crabtree JS, Scacheri PC, Ward JM, McNally SR, Swain GP, *et al.* (2003) Of
324   mice and MEN1: Insulinomas in a conditional mouse knockout. *Mol Cell Biol*
325   23: 6075-6085.

326   26. Johansen T, Lamark T. (2011) Selective autophagy mediated by autophagic
327   adapter proteins. *Autophagy* 7: 279-296.

328   27. Shi J, Fung G, Deng H, Zhang J, Fiesel FC, *et al.* (2015) NBR1 is dispensable
329   for PARK2-mediated mitophagy regardless of the presence or absence of
330   SQSTM1. *Cell Death Dis* 6:e1943.

331   28. Murakawa T, Yamaguchi O, Hashimoto A, Hikoso S, Takeda T, *et al.* (2015)
332   Bcl-2-like protein 13 is a mammalian Atg32 homologue that mediates
333   mitophagy and mitochondrial fragmentation. *Nat Commun* 6:7527.

334   29. Bhujabal Z, Birgisdottir ÅB, Sjøttem E, Brenne HB, Øvervatn A, *et al.* (2017)
335   FKBP8 recruits LC3A to mediate Parkin-independent mitophagy. *EMBO Rep*
336   18:947-961.

337   30. Cui Y, Huang L, Elefteriou F, Yang G, Shelton JM, *et al.* (2004) Essential role
338   of STAT3 in body weight and glucose homeostasis. *Mol Cell Biol* 24: 258-269.

339   31. Ebato C, Uchida T, Arakawa M, Komatsu M, Ueno T, *et al.* (2008) Autophagy
340   is important in islet homeostasis and compensatory increase of beta cell mass in
341   response to high-fat diet. *Cell Metab* 8: 325-332.

342

343   **Figure legends**

344

345   **Fig. 1 Expression of *p62* in beta-cell specific *p62*-knockout mice**

346   Quantitative real-time PCR analysis of p62 in *p62$^{+/+}$:RIP-Cre* (*p62$^{+/+}$:Cre*) and

347   *p62$^{f/f}$:RIP-Cre* (*p62$^{f/f}$:Cre*) islets. mRNAs were prepared from islets of mice with the

348   indicated genotypes at 24 weeks of age. Values were normalized to the amount of

349   mRNA in *p62$^{+/+}$:Cre* islets. Expression levels of p62 mRNAs were decreased by more

350   than 70% in islets of *p62$^{f/f}$:Cre* mice (n = 3 each, *$p < 0.001$). Data are the mean ±

351   SEM.

352

353

354   **Fig. 2 Ablation of p62 in β cells does not lead to body weight gain nor to**

355   **differences in non-fasting blood glucose levels**

356   Changes in body weight (A) and non-fasting blood glucose levels (B) of *p62$^{+/+}$:Cre*

357   (blue circles; n = 10), *p62$^{f/+}$:Cre* (green circles; n = 10), and *p62$^{f/f}$:Cre* (red circles; n =

358   10) mice between 6 and 22 weeks of age. Data represent the mean ± SEM.

359

Fig. 3 Ablation of p62 in β cells does not exacerbate glucose tolerance

Blood glucose concentrations (A) and serum insulin levels (B) measured during

IPGTT at the age of 22 weeks. Blue circles, $p62^{+/+}$:*Cre* mice (n = 10); green circles,

$p62^{f/+}$:*Cre* mice (n = 10); and red circles, $p62^{f/f}$:*Cre* mice (n = 10). Data represent the

mean ± SEM.

365

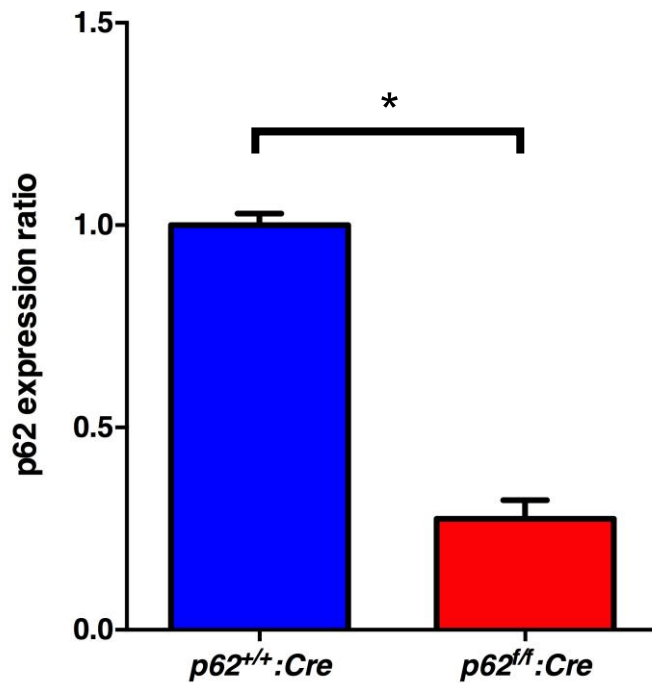**Fig. 4 Ablation of p62 in islets does not result in morphological abnormalities of islets**

(A) Representative images of hematoxylin and eosin staining of islets of 22-week-old

$p62^{+/+}$:*Cre*, $p62^{f/+}$:*Cre*, and $p62^{f/f}$:*Cre* mice. Scale bars represent 100 μm.

(B) Representative images of insulin staining of the islets of 22-week-old $p62^{+/+}$:*Cre*,

$p62^{f/+}$:*Cre*, and $p62^{f/f}$:*Cre* mice. Scale bars represent 100 μm.

(C) Percent islet area of $p62^{+/+}$:*Cre* (n = 4), $p62^{f/+}$:*Cre* (n = 5), and $p62^{f/f}$:*Cre* mice

(n = 6). Data represent the mean ± SEM.

373
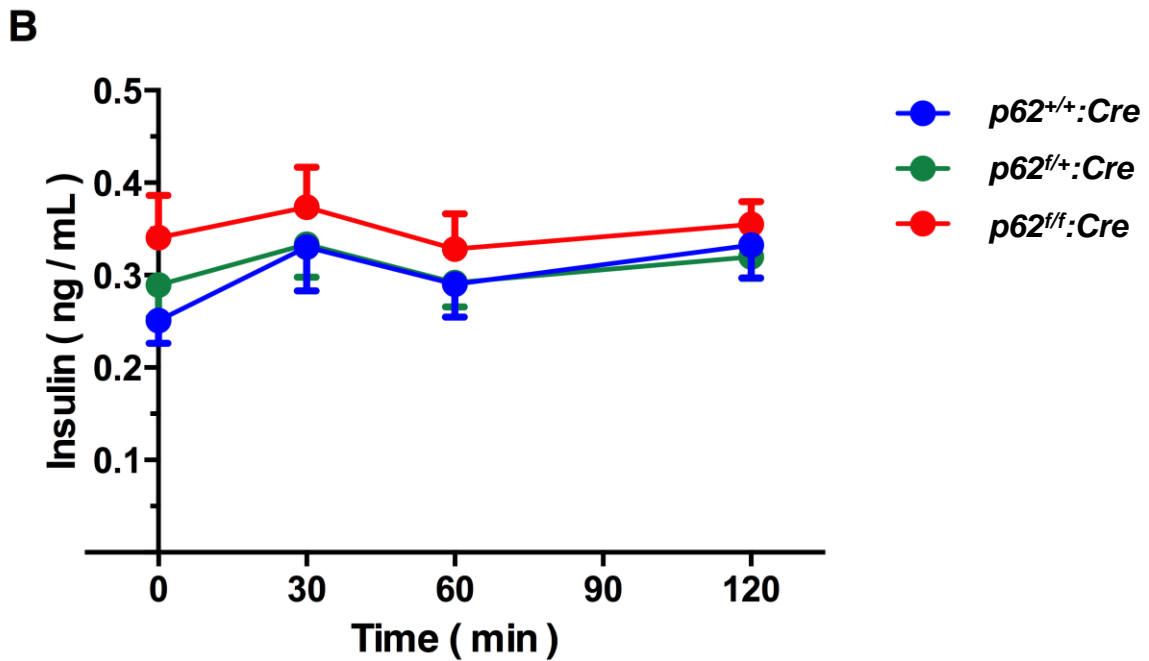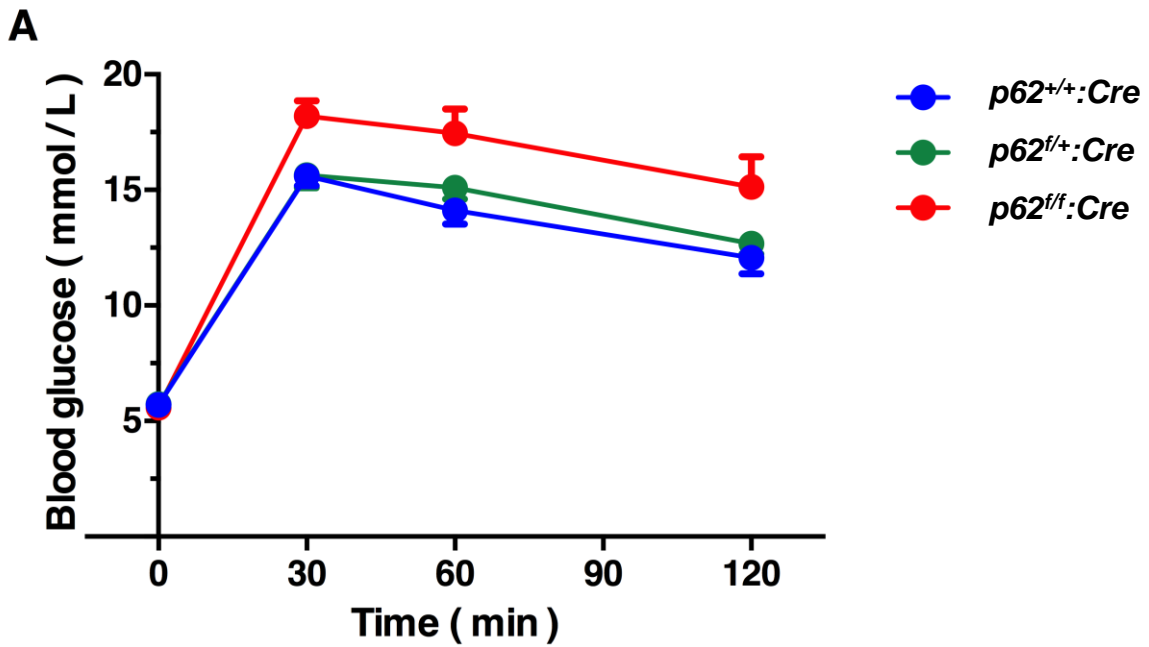
Fig. 1 Expression of *p62* in beta-cell specific *p62*-knockout mice
Quantitative real-time PCR analysis of *p62* in *p62+/+:RIP-Cre*
(*p62+/+:Cre*) and *p62f/f:RIP-Cre* (*p62f/f:Cre*) islets. mRNAs were
prepared from islets of mice with the indicated genotypes at 24 weeks
of age. Values were normalized to the amount of mRNA in *p62+/+:Cre*
islets. Expression levels of *p62* mRNAs were decreased by more than
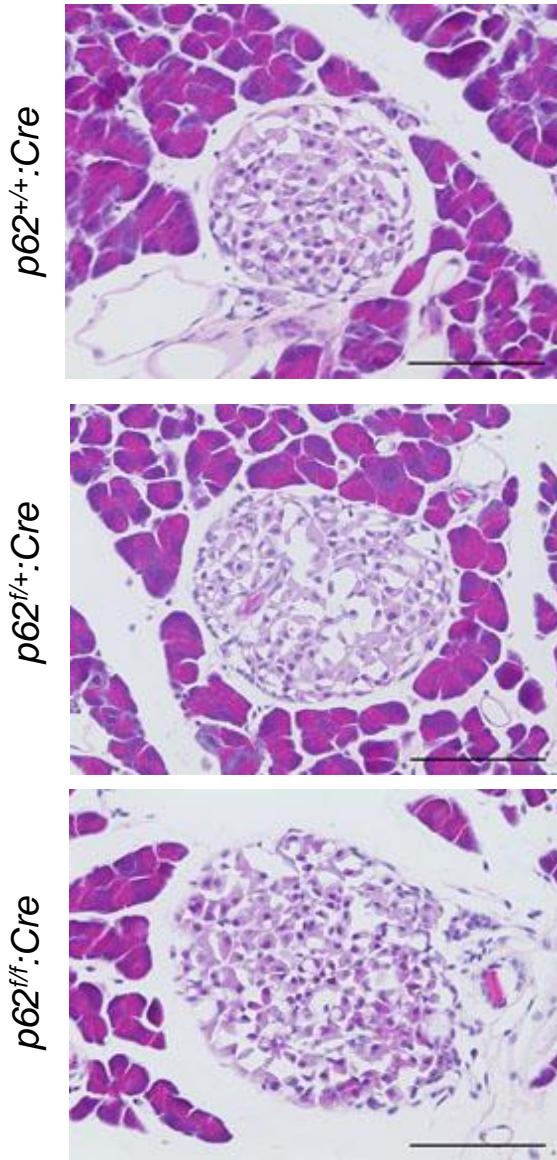70% in islets of *p62f/f:Cre* mice (n = 3 each, *$p < 0.001$). Data are the
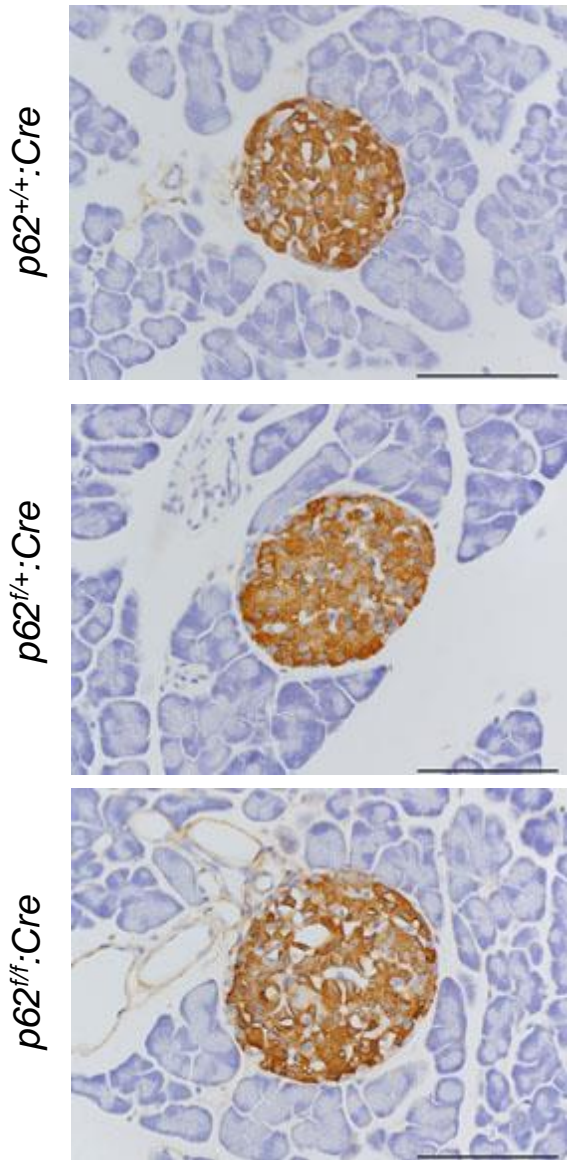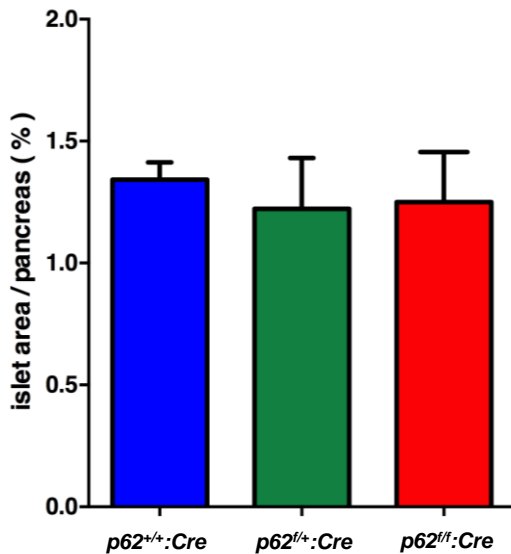mean ± SEM.

A

B
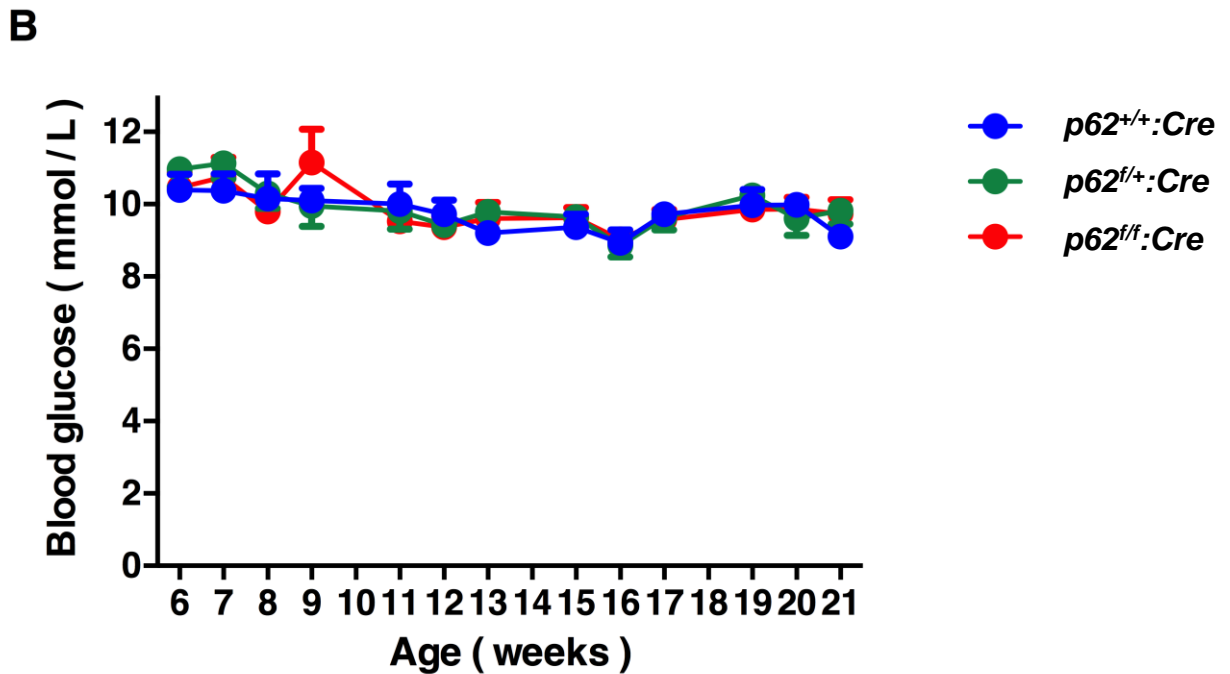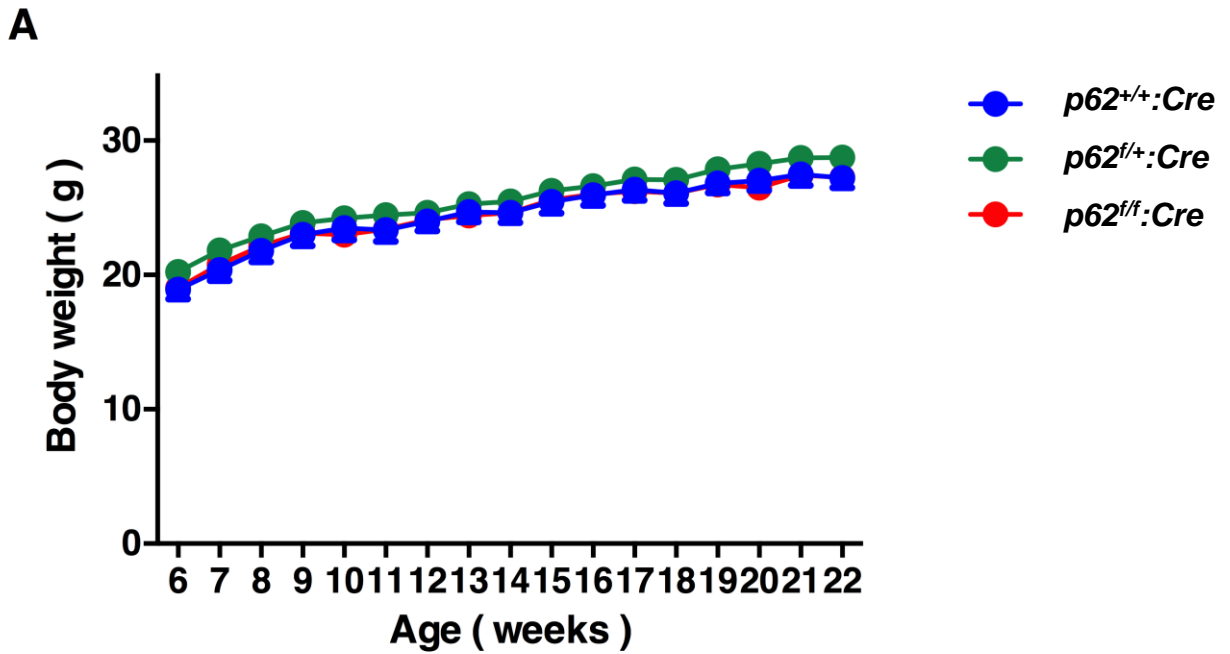
Fig. 2 Ablation of *p62* in β cells does not lead to body weight gain nor to differences in non-fasting blood glucose levels
Changes in body weight (A) and non-fasting blood glucose levels (B) of *p62⁺/⁺:Cre* (blue circles; n = 10), *p62^{f/+}:Cre* (green circles; n = 10), and *p62^{f/f}:Cre* (red circles; n = 10) mice between 6 and 22 weeks of age. Data represent the mean ± SEM.

Fig. 3 Ablation of p62 in β cells does not exacerbate glucose tolerance
Blood glucose concentrations (A) and serum insulin levels (B) measured during IPGTT at the age of 22 weeks. Blue circles, *p62+/+:Cre* mice (n = 10); green circles*, p62f/+:Cre* mice (n = 10); and red circles, *p62f/f:Cre* mice (n = 10). Data represent the mean ± SEM.

A

p62+/+:Cre

p62f/+:Cre

p62f/f:Cre

B

p62+/+:Cre

p62f/+:Cre

p62f/f:Cre

C

Fig. 4 Ablation of *p62* in islets does not result in morphological abnormalities of islets

(A) Representative images of hematoxylin and eosin staining of islets of 22-week-old *p62+/+:Cre*, *p62f/+:Cre*, and *p62f/f:Cre* mice. Scale bars represent 100 μm.

(B) Representative images of insulin staining of the islets of 22-week-old *p62+/+:Cre*, *p62f/+:Cre*, and *p62f/f:Cre* mice. Scale bars represent 100 μm.

(C) Percent islet area of *p62+/+:Cre* (n = 4), *p62f/+:Cre* (n = 5), and *p62f/f:Cre* mice (n = 6). Data represent the mean ± SEM.